Journal of African Earth Sciences 111 (2015) 421–433

Contents lists available at ScienceDirect

Journal of African Earth Sciences

journal homepage: www.elsevier.com/locate/jafrearsci

Geological setting, emplacement mechanism and igneous evolution of the Atchiza mafic-ultramafic layered suite in north-west Mozambique

Daniel Luis Ibraimo [a, b, *], Rune B. Larsen [a]

[a] Department of Geology and Mineral Resources Engineering, Norwegian University of Science and Technology, Trondheim, Norway
[b] Departamento de Geologia, Faculdade de Ciências, Universidade Eduardo Mondlane, Maputo, Mozambique

ARTICLE INFO

Article history:
Received 21 March 2015
Received in revised form
20 July 2015
Accepted 21 July 2015
Available online 1 August 2015

Keywords:
Atchiza
Mafic
Ultramafic
Layered intrusion
Emplacement mechanism
Zambezi belt

ABSTRACT

The Atchiza mafic and ultramafic-layered suite (hereafter, "Atchiza Suite) crops out in an area 330 km^2 west of the Mozambican Tete province. In an early account of the geology of this intrusion, it was considered the continuation of the Great Dyke of Zimbabwe, an idea that was aborted after detailed studies. Nevertheless, the Ni concentrations in the Atchiza outcrop rocks are considerable. Our investigation used field evidence, hand specimens and petrography descriptions, mineral chemistry studies using electron microprobe analysis and tectonic analysis to arrive at a plausible mineralogical composition and understanding of the tectonic setting for the igneous evolution. The mineral composition from the Atchiza Suite indicates that these are cumulates. The magmatic segregation from the petrographic and mineral composition reasoning indicates that dunite-lherzolitic peridotite-olivine gabbro-gabbronorite-gabbro-pegmatitic gabbro is the rock formation sequence. Olivine and chromite were the first phases formed, followed by pyroxene and plagioclase. In addition, it is shown that these minerals are near-liquidus crystallization products of basaltic magma with olivine Fo: 87.06 in dunite, mean values of clinopyroxene are (Wo: 36.4, En: 48.0, Fs: 15.2), orthopyroxene (Wo: 2.95, En: 73.0, Fs: 24.2) and plagioclase An: 71.3, respectively. Opaque minerals comprise Fe–Ti oxides and (Fe, Cr) spinel up to 4.8 vol.%, but chromitite layers are not present. Most of the opaque minerals are interstitial to pyroxene. Sulphides are common in gabbros, with pyrrhotite, pentlandite, chalcopyrite, pyrite and covellite together comprising 0.4–2.0 vol.%. The whole rock Rare Earth Element (REE) concentrations are mainly a result of differentiation, but slight crustal contamination/assimilation contributed to the REE contents. In addition, they also show Eu enrichment, suggesting that plagioclase fractionation was important in the rock. The Atchiza Suite preserves a deep-seated plumbing system of the continental rift environment. The intrusion resulted from the emplacement of mafic magma in space created by extensional forces. Space was created through a connecting fault generated as a result of overall extensional, torsion and slab displacement in a rift system. The geometry of the body is tectonically controlled, and it agrees with the tectonic framework of the Zambezi Belt during the Rodinia breakup in the early Neoproterozoic.

1. Introduction

Mafic and ultramafic rocks of considerable size become fundamental targets because of their hidden economic value. There are many cases of thorough investigations on mafic and ultramafic rocks related to Ni–Cu sulphides and Platinum Group Elements (PGE) deposits. The occurrence of these types of rocks has been related to large layered igneous intrusions and intracratonic magma conduit emplacements through sutures where extension and rifting are limited.

Mineral resources are valueless when unexplored and unexploited. To reach the stage of exploitation, geological knowledge and understanding the minerals' characteristics has become imperative. Many papers published in recent years (e.g., Ferreira Filho et al., 2010; Pereira et al., 2014; Maier and Groves, 2011) have dealt with revealing geological characteristics and the emplacement of mafic and/or ultramafic intrusions that host Ni–Cu and PGE deposits. Here, new results are presented by studying the Atchiza Suite. The results are comprised of understanding the properties and characteristics of these rocks in the setting of the ore deposit formation.

* Corresponding author. Department of Geology and Mineral Resources Engineering, Norwegian University of Science and Technology, Trondheim, Norway.
E-mail addresses: daniel.ibraimo@ntnu.no, daniel.ibraimo@gmail.com (D.L. Ibraimo), rune.larsen@ntnu.no (R.B. Larsen).

http://dx.doi.org/10.1016/j.jafrearsci.2015.07.020
1464-343X/

Mafic-ultramafic rocks are not common in the Zambezi Belt, although they occasionally appear in the Tete Province (Mozambique), e.g. the Tete gabbro-anorthosite suite and the Chipera gabbro-anorthosite intrusion. Contrary to the Atchiza Suite, they are older (ca. 1005 Ma), formed in a different tectonic regime and have experienced more deformation (Evans et al., 1999; Westerhof et al., 2008).

The Atchiza Suite is often targeted for its mineral potential. The first detailed study of the Atchiza Suite was done by Vasconcelos & Hall (1948), who described the mafic-ultramafic rocks for the first time. These studies were followed up in 1955 by a team of geologists from the Longyear Company. The results of these early studies were only published in 1962. Real (1962) published another report on the intrusion, introducing the hypotheses that the Atchiza intrusion was a continuation of the Great Dyke of Zimbabwe. This was based on the geographic position and the geology of both intrusions. He also described chromite and asbestos found in the Great Dyke and Atchiza Suite to support his hypotheses. However, after detailed petrographic and chemical analyses, it was concluded that the Atchiza Suite deviated significantly from the Great Dyke of Zimbabwe, and their connectivity was abandoned (GTK Consortium, 2006).

The Atchiza Suite was mapped in detail by Hunting Geology and Geophysics Studies from 1982 to 1983, which was followed by data processing and interpretation by Anglo American in 1991. The GTK Consortium later remapped the intrusion on a 1:250,000 scale and conducted geochronology and geochemistry investigations from 2003 to 2006 (GTK Consortium, 2006; Westerhof et al., 2008).

Qualitative resource assessment and mineral potential studies show that the Atchiza Suite hosts Ni–Cu sulphides, Fe–Ti oxides, ferrichromium spinel and chromite mineralisations associated with the ultramafic rocks. Disseminated chromite occurs as a primary mineral formed during fractional crystallization with primary magnetite and olivine, but chromitite layers are absent.

All these previous studies were aimed at finding economic ore-deposits, not at understanding the origin and evolution of the intrusion. Therefore, this paper aims to provide the first comprehensive and scientific understanding of the geology, petrology, emplacement mechanism and igneous evolution of the intrusion.

2. Materials and methodology

2.1. Materials

Fresh samples are difficult to obtain in the field due to varying degrees of weathering. Fig. 1 shows examples of the alteration status of the best samples (16 in total) used in this study. The left figure (i.e., Fig. 1-A) was taken from an unaltered fine-grained olivine gabbro, and the right (i.e., Fig. 1-B) shows slightly altered peridotite. Used samples represent six different rock types: dunite, lherzolitic peridotite, olivine gabbro, gabbronorite, gabbro and pegmatitic gabbro, distinguished by their petrographic and mineral geochemistry characteristics. The selected samples cover the entire range of lithologies present in the study area.

2.2. Electron probe micro-analyser (EPMA)

Thin and polished sections with ~270 Å carbon coating were loaded into a JEOL JXA-8500F thermal field emission electron probe micro-analyser located at the laboratory of the Department of Material Science and Engineering at NTNU. The instrument is equipped with five Wavelength Dispersive Spectrometers (WDS) and one Energy Dispersive Spectrometer (EDS), allowing simultaneous acquisition of $5 + 16$ elements. The instrument was operated at 10^{-5} Torr or better, at an accelerating voltage of 15 kV, 20 nA beam current, and 250 ms dwell time, with an effective beam diameter of ~1 μm (i.e., current density >25 nA/μm^2). Only one visiting time was performed for each programmed view, and the data were provided as element and oxide maps.

In 16 least altered and representative samples, which also were minimally altered, 568 spot analyses were carried out, of which, 292 were in olivine, 75 in pyroxene and plagioclase, 189 in oxides, 12 in sulphides and the remaining in biotite, chlorite, zircon and apatite.

3. Regional framework and structural-tectonic setting

The Atchiza mafic and ultramafic intrusion is located in the Zambezi Belt, which is a mosaic of juxtaposed terranes with contrasting structural and tectonic histories. The Zambezi Belt experienced two major tectonic events in the Mesoproterozoic to Neoproterozoic: (1) the breakup of Rodinia (continental rifting) and, (2) the assembly of Gondwana (continental collision and subsequent amalgamation). These two tectonic events are described by Johnson and Oliver (2004). They analysed the Southern African Cratons of the Mesoproterozoic Rodinia supercontinent, including the possible timing constraints for the breakup and subsequent Neoproterozoic (including the Pan-African orogeny) continental collision and amalgamation of Gondwana. Further, Stern (1994) correlated both tectonic events with the large structure associated with the East Africa Orogeny; Dirks and Sithole (1999) mostly studied the continental collision; Westerhof et al.

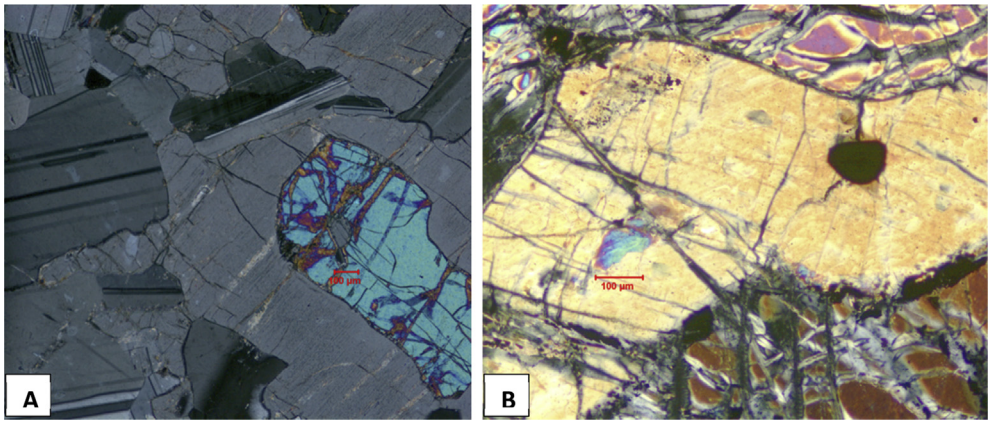

Fig. 1. Photomicrography of two different minerals status: A-Fine-grained olivine gabbro→Non-Altered; B-Lherzolitic peridotite→Moderate-Altered.

(2008) studied three lithospheric plates comprising East, West and South Gondwana that are sutured in the Tete-Chipata Belt.

The Zambezi Belt is regarded as a continuous orogenic belt stretching from the Mozambique Belt in the East (corresponding to East Gondwana) to the Irumide Belt in the West (West Gondwana). However, the full structural-tectonic setting is not fully understood because the Zambezi Belt largely is composed of reworked, pre-Pan-African to late Neoproterozoic basement gneisses (Goscombe et al., 2000).

The emplacement of the Atchiza Suite is better explained after a full analysis of the structural-tectonic framework of the Zambezi Belt.

3.1. Rodinia breakup

The Zambezi Belt resulted from Rodinia intracontinental rifting, as shown in many parts of the Zambezi Belt where rifting characteristics are reported in the Damara Belt and Lufilian Arc (Porada, 1989). Rifting in the given area started around 1350 Ma and continued up to 750 Ma (Goscombe et al., 2000). In the central north-west Mozambique, rifting is evidenced by the Zambezi Fault and the Fínguè Shear Zone. This zone bordering the study area to the north comprises an ensialic basement structurally overlain by thick supracrustal rocks including extension related bimodal volcanic suites recorded as initial extensional magmatism along the fault and overlain by clastic sediments (Fig. 2). The Fínguè supercrustal rocks comprise a narrow section, approximately 150 km long located between deformed granitic gneisses and granitoids. Rifting related rocks are comprised of felsic meta-volcanics, ignimbrites and volcanic breccias with a Mesoproterozoic age of 1327 ± 16 Ma (magmatic U–Pb age from GTK Consortium, 2006) mainly found together with metasedimentary rocks of the eastern tip of the Fínguè Fault. Younger felsic meta-volcanic rocks and meta-tuffs of late Mesoproterozoic age 1050 ± 8 Ma (U–Pb zircon age; GTK Consortium, 2006) are also present in the Fínguè Supergroup.

Based on the above geochronology of felsic and mafic volcanic rocks in the Fínguè Supergroup, it is concluded that the tectonic evolution began 1350 Ma and continued to 750 ± 17 Ma before continental collision. Similar ages are found in the supracrustal rocks from southern Zambia, which contain basal meta-rhyolites dated at 879 ± 19 Ma (U–Pb zircon age; GTK Consortium, 2006 and references therein), all of which can be attributed to the same tectonic events. The Fínguè Fault started as a normal fault and was associated with the major events occurring along the Zambezi Belt. The bimodal volcanic rock sequence in the Fínguè Fault zone may be interpreted to record extension-related magmatism associated with rifting episodes.

3.2. Gondwana phase

Rifting in the Zambezi Belt ceased and was followed by continental collision and amalgamation during the Pan-African Orogeny; i.e. the Fínguè Fault Zone experienced an amalgamation of crust during the Pan-African episode. Through amalgamation, the east and west Gondwana assembled in a thrusting regime with north-northwest nappe emplacement (Stern, 1994; Kröner and Stern, 2004; Johnson and Oliver, 2004). High-pressure metamorphic rocks, including eclogites, are scattered along the entire length of the Zambezi Belt from south Malawi to northeast Zimbabwe (i.e., the Makuti Group; Dirks and Sithole, 1999) and within the Zambezi supracrustals in the Lusaka area, Zambia (Goscombe et al., 2000). They imply the closure of an ocean basin in a crustal suture. This is also evidenced by the presence of relict oceanic crust, i.e. ophiolite (Oliver et al., 1998).

Then, continental collisional and orogenesis in the Zambezi tectonic zone continued throughout the Pan-African orogeny (Gondwana assembly) in mid to late Neoproterozoic (740–540 Ma).

4. Geology and petrography

4.1. Geological setting

The mafic-ultramafic rocks of the Atchiza Suite comprise an intrusive body in the Fínguè Supergroup at the western tip of the Fínguè shear zone (Fig. 3). The intrusion has sharp contacts with the

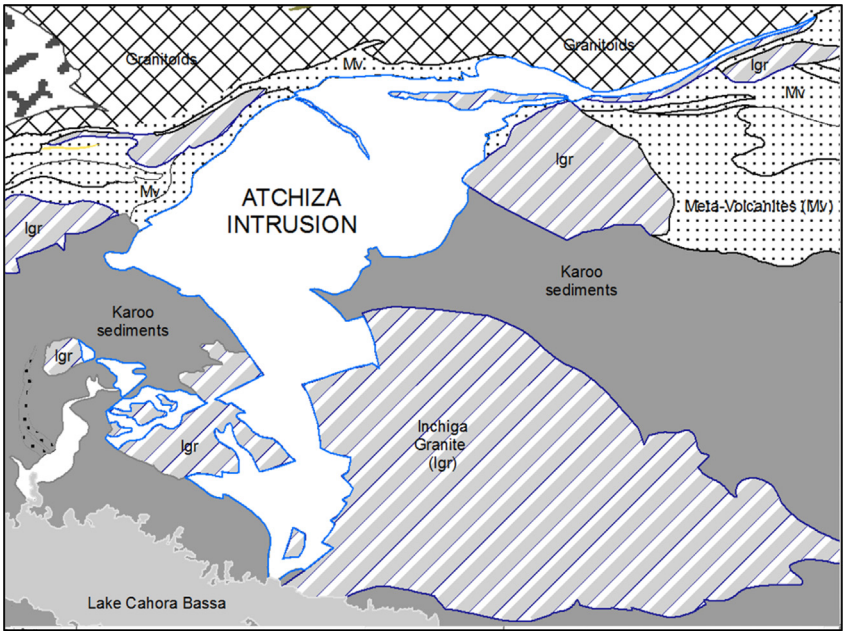

Fig. 2. Sketch of the Atchiza mafic-ultramafic Suite and its relationship with the country rocks, adapted after geology map produced by GTK Consortium (2006).

country rock towards the west and also with the Fínguè Shear Zone in the north. In the east and south-west, it is covered by the Phanerozoic Karoo formations.

The country rocks include gneisses, meta-volcanics and meta-sedimentary lithologies along the northern contact throughout the Fínguè Shear Zone, syn-tectonic granites and granodiorites and the Karoo Phanerozoic cover. The Atchiza body is intrusive with respect to Inchinga granite (Fig. 3). Their structural and field relations are in agreement with the age determination obtained by Ibraimo and Jamal in preparation.

The lowermost portion of the Atchiza Suite comprises an ultramafic succession of dunites and lherzolitic peridotites (partially serpentinised), which are also found in the west and north-west ends of the intrusion. These are overlain by a gabbroic sequence comprising olivine gabbros, gabbronorites, gabbros and pegmatitic gabbros. The gabbros partly exhibit traces of hydrothermal alteration and are affected by metamorphism (Meta-gabbros). The gabbroic sequence progressively changes from fine to coarse-grained gabbros to pegmatitic gabbro. The central segment of the gabbroic succession comprises pegmatitic gabbros with plagioclase crystals ranging from 3 to 6 cm. Gabbroic rocks comprise most of the Atchiza Suite followed in abundance by dunites and lherzolitic peridotites, especially along the western limit and central-southern areas.

The country rock, Inchiga granite, is segmented into a number of blocks and intruded by the Atchiza body (Figs. 3 and 9C). The granite is light grey to pink with medium-to coarse-grained crystals of porphyritic microcline. The porphyritic granite is progressively more deformed towards the shear zone (Fig. 3), and the primary porphyric grains remain recognisable. Xenoliths of well-preserved quartzite, meta-arkose and meta-volcanite are common in the granite. Bimodal meta-volcanites are common along the Fínguè Shear Zone towards the northern limit of the Atchiza intrusion (GTK Consortium, 2006). These rocks are part of Monte Rupanjaze and the Monte Muinga Formations, comprised of mafic, felsic and intermediate meta-volcanites and mica-schist.

4.2. Petrography of silicates and opaque minerals

4.2.1. Silicates

Cumulus gabbros are composed of fine to pegmatitic-grained clinopyroxene (diopside, augite and endiopside), orthopyroxene (En 65.78 to 68.37) and plagioclase (An 87–60, when cumulus crystals) being ca-rich (Bytownite and Labradorite) or (An 60–55 when interstitial or as chada-crysts in pyroxenes) being more sodic rich (Andesine) (Fig. 4-B). Locally, flakes of biotite with weak pleochroism were found, which are associated with altered rims of pyroxenes together with secondary opaque minerals. Accessory phases include olivine and rare amphibole. Opaque minerals are concentrated in fine-to coarse-grained gabbros. Compositionally, the gabbroic rocks are classified as gabbronorites and gabbros (Streckeisen, 1976). Ophitic and sub-ophitic intergrowth of bytownite-labradorite and augite are common.

Dunites are >95% olivine (Fo 86.55–87.06) primocrysts and a matrix of intercumulus clinopyroxene (diopside). Lherzolitic peridotite is composed essentially of medium-grained cumulus olivine (forsterite) and clinopyroxene (diopside and endiopside; Fig. 4-B) with rare plagioclase. The matrix comprises clinopyroxene (augite) and orthopyroxene (bronzite) and sometimes plagioclase. The modal composition of the rock is 75% olivine, 23% clinopyroxene and 1.4% opaque minerals. This is the case when olivine is abundant, but with a lower percentage of olivine, the modal composition is 50% olivine, 32% orthopyroxene, 16% clinopyroxene with 1% amphibole and less than 1% opaque minerals. Some minor alteration minerals are common. Biotite, together with opaque matter, is associated with the alteration of clinopyroxene. Secondary chlorite and magnesite are also observed. Serpentinites pseudomorphing primocryst of olivines are common in the northern segment of the Atchiza Suite towards the Fínguè Shear Zone.

Earlier work reports pyroxenite in the Atchiza Suite (GTK Consortium, 2006). However, closer inspection of the supposed pyroxenite shows that cumulus plagioclase comprises >20%. Consequently, these rocks have been reclassified as gabbronorites or, in places, olivine gabbro.

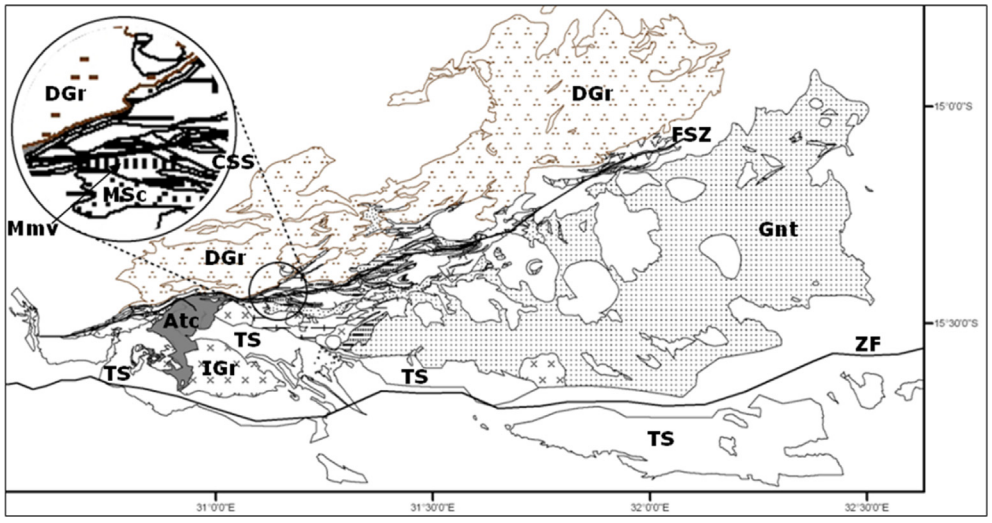

Fig. 3. Geology of the Fínguè Supergroup and adjacent rock formations, Northwest Tete Province, Mozambique. labels: **Atc** = Atchiza Suite, **DGr** = Megacrystic, deformed granite and granitoids, **FSZ**= Fínguè Shear Zone, **Gnt** = Granitoids, medium-coarse granite, deformed, **IGr** = Inchinga Granite, porphyritic, **TS** = Phanerozoic sediments, sandstone, **ZF** = Zambezi Fault. **Zoomed Circle**: **CSS**=Calc-Silicate gneiss and Schist. **Mmv** = Mafic and Ultramafic metavolcanic rock, **MSc** = Mica Schist & mica gneiss. Modified after geology map produced by GTK Consortium (2006).

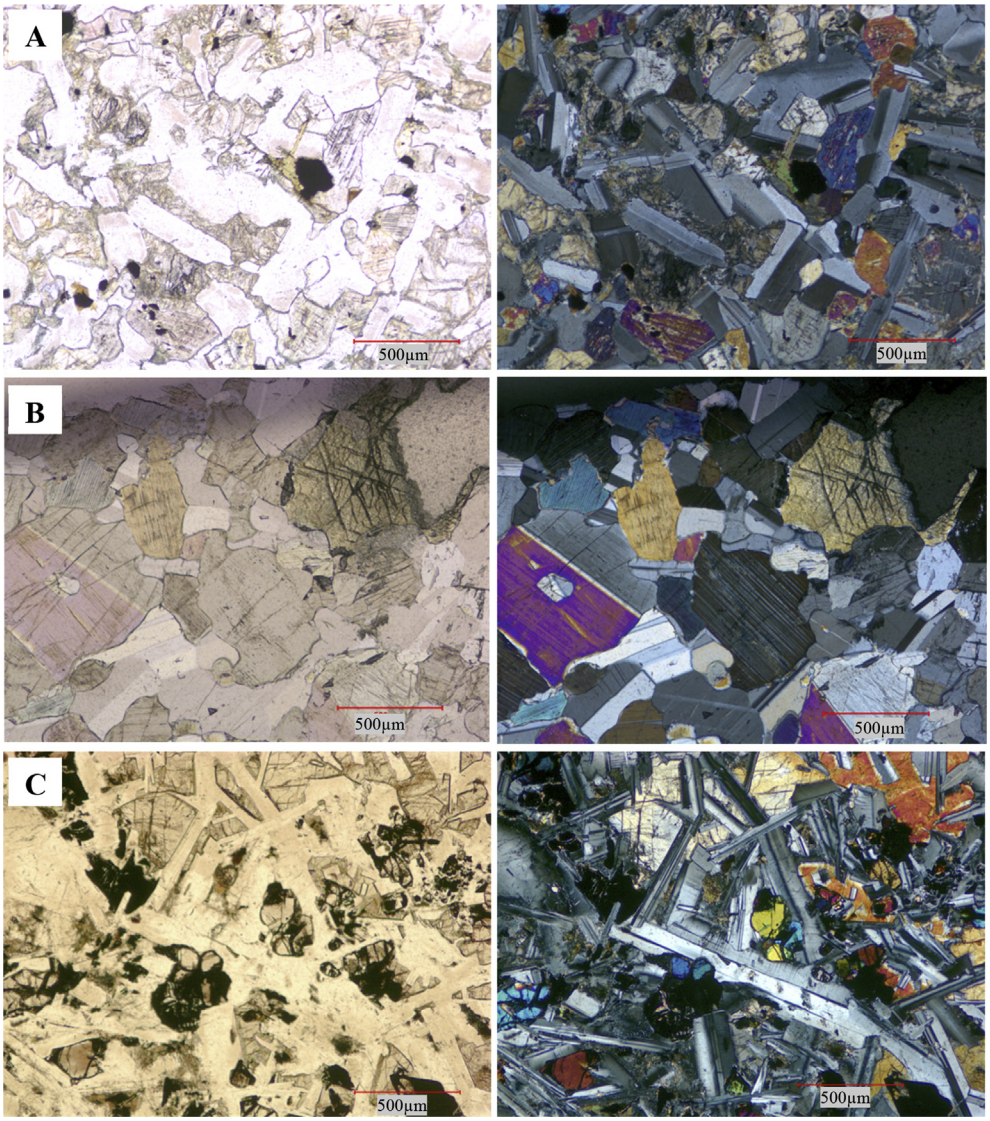

Fig. 4. Gabbro microphotograph of the Atchiza Intrusion. A-fine-grained gabbronorite with ophitic texture, the cumulate minerals are clinopyroxene and plagioclase in a matrix of intercumulate orthopyrone; B-medium-grained gabbronorite with augite and Labradorite-Bytownite as cumulate minerals; C-subophitic texture on olivine gabbronorite with poikilitic clinopyroxene and olivine growing in between large plagioclase crystals.

Coarse and pegmatitic gabbros are spatially located in the centre of the gabbroic suite. The rock type is fairly altered, but it is possible to observe relicts of pyroxene and plagioclase. The pegmatitic gabbro is associated with the main cumulus sequence of the Atchiza gabbroic rocks. It comprises coarse to pegmatitic clinopyroxene (augite) as the main cumulus phase together with plagioclase (An 59.01–64.55), also occasionally with large tabular crystals up to 1 cm. The intercumulus assemblage comprises an intergrowth of quartz, biotite and Fe–Ti rich oxides, which enclose the clinopyroxene. Clinopyroxene and plagioclase are ophitic with olivine and Fe–Ti rich oxide inclusions.

4.2.2. Opaque minerals

Opaque phases are common. Sulphides are particularly common at the northern contact towards the Fínguè Shear Zone and in specific lithologies of the mafic-ultramafic Suite. The opaque phases are comprised of Fe–Ti oxides (0.8–4.8 vol.%), mostly magnetite, ilmenite and (Fe, Cr) spinel. Magnetite occurs as anhedral semi-rounded crystals. Magnetite in dunite and lherzolitic peridotite is subhedral and medium-grained, mostly occurring in the groundmass and in olivine fractures. In addition, secondary magnetite (e.g., in fractures in olivine) is very common during serpentinisation. Ilmenite occurs as homogeneous subhedral grains. The (Fe, Cr) spinels are euhedral fine-grained (up to 300 μm), cubic to subrounded in shape. The ferrrichromite minerals predominate in the interstices enclosing olivine primocrysts in dunite and lherzolitic peridotite rocks. In addition, chromite is found as intergrowth at the boundaries with olivine. Mostly, they are interstitial with pyroxene, but some are inclusions in olivine grains, which suggests that chromite formed simultaneously and posterior to olivine (Chai and Naldrett, 1992).

Sulphides comprise pyrrhotite, pentlandite, chalcopyrite, pyrite and covellite in gabbroic rocks (0.4–2.0 vol.%). They occur either as disseminated grains or as specks adjacent to each other (Fig. 5). Pyrrhotite forms the largest grains in the gabbroic suite with crystals up to 500 μm and, in many cases, with pentlandite laths that apparently exsolve from the larger masses.

Chalcopyrite is one of the common sulphides in the Atchiza

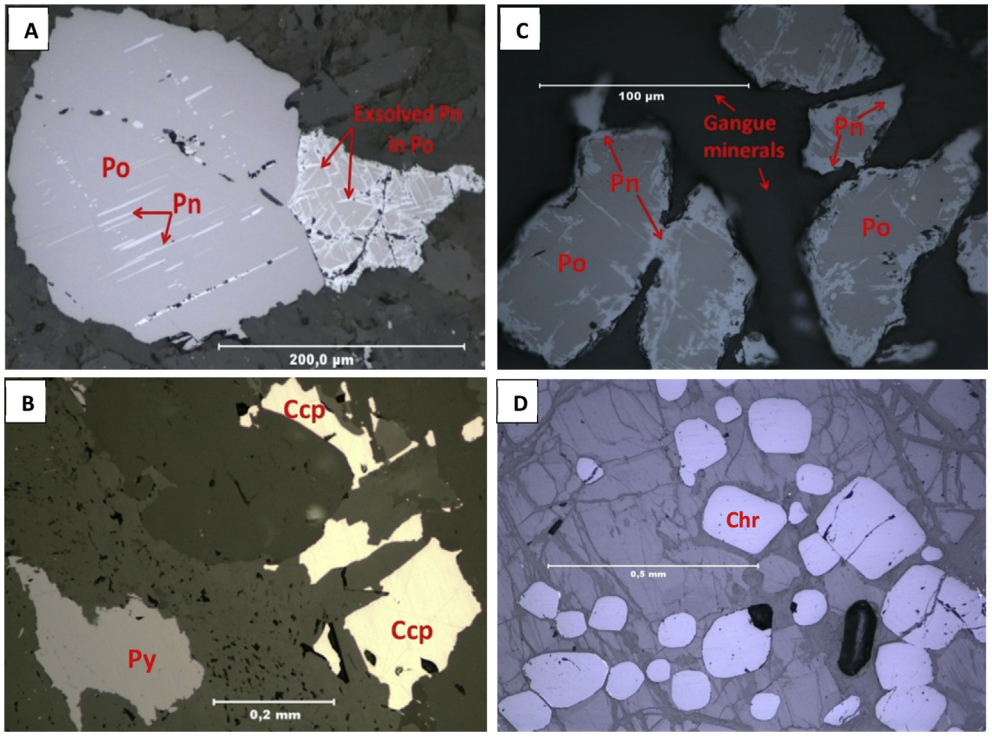

Fig. 5. Microphotographs of opaque minerals from the Atchiza Intrusion. A – Pyrrhotite and exolved pentlandite in a gabbro rock; B – Most common sulphides in the intrusion (Chalcopyrite and pyrite); C – Pentlandite reaming the borders and exolved in Pyrrhotite. D – Ferrichromite fine subhedral and subrounded grains in dunite.

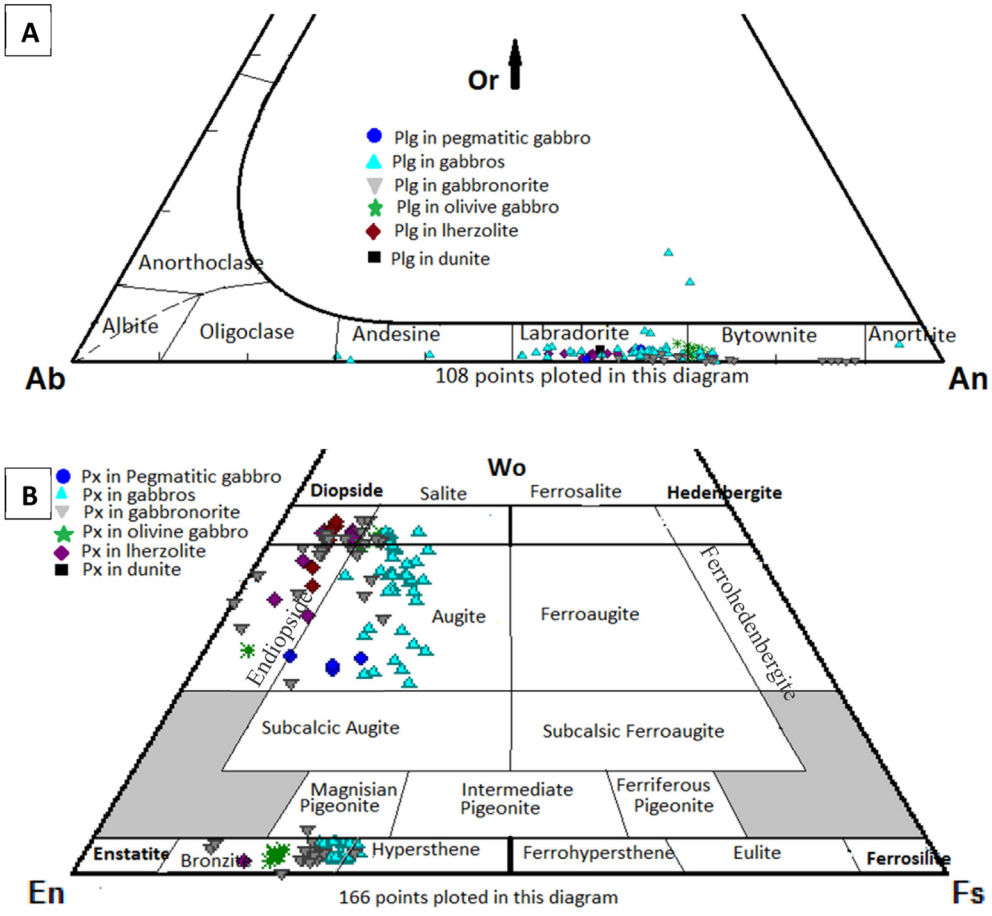

Fig. 6. Distribution diagrams and their appropriate names: A- Plagioclase, B- Pyroxenes of the mafic-ultramafic rocks of the Atchiza Intrusion.

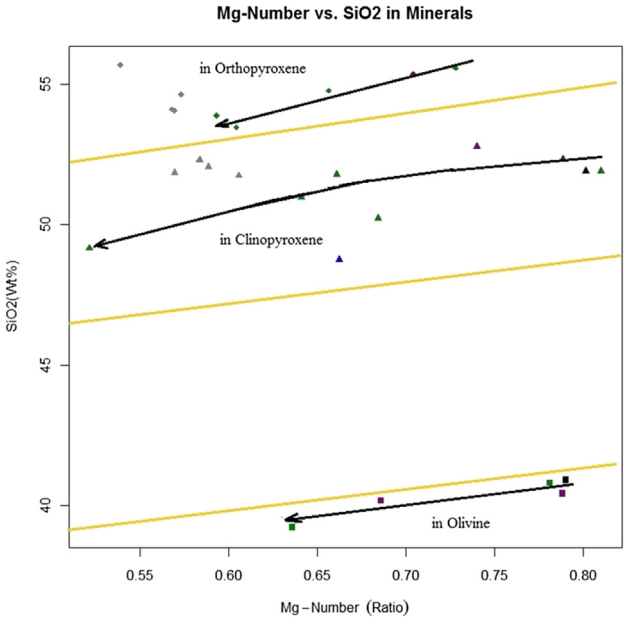

Fig. 7. Mineral composition trends from ultramafic to mafic rocks. Colour scheme is: black-dunite, purple-lherzolite, green-gabbronorite, grey-gabbro and blue-pegmatitic gabbro. Yellow lines separate the fields of minerals. (For interpretation of the references to colour in this figure legend, the reader is referred to the web version of this article.)

Suite (Fig. 5). It often occurs together with pyrite exhibiting subhedral and anhedral forms. Both minerals occur as intercumulus phases in the gabbroic rocks. In deformed rocks, from the contact between the mafic-ultramafic and country rocks, associated with the shear zone, chalcopyrite-pyrite grows as phenocrysts in rock fractures, which may result from fluid recrystallization. Covellite is found in limited abundance with remnant chalcopyrite in the centre suggesting it is the result of the pseudomorphic replacement of chalcopyrite. It is deep blue to sky-blue in colour and anhedral to euhedral. In lherzolite, sulphides are interstitial; they typically occur in the middle of the interstitial voids, with interstitial pyroxene and plagioclase separating them from the cumulus olivine and clinopyroxene.

5. Mineral chemistry

Microprobe analyses were carried on 16 selected samples consisting of one dunite, two lherzolitic peridotites, two olivine gabbro, three gabbronorites, five gabbros and one pegmatitic gabbro. Results from the olivine are presented in Table 1, and show SiO_2 contents ranging from 39.2 to 40.9 W t%, FeO from 12.28 to 22.14 W t% and MgO from 28.64 to 46.15 W t%. The forsterite content is 86.8 in Dunite, 86.7 in high olivine lherzolite, 79.3 in low olivine lherzolite and 75.4–86.2 in gabbros. Pyroxenes from the Atchiza Suite are dominated by clinopyroxene with a minor proportion of orthopyroxene. Clinopyroxene analyses are given in Table 2. Following the classification by Poldervaart and Hess (1951) Clinopyroxenes mostly classify as augite, diopside and endiopside (Wo: 27.5–45.2, En: 40.3–55.6, Fs: 6.2–24.2) (Fig. 6-B). Diopside occurs in dunite lherzolitic peridotite with high olivine contents. The CaO content ranges from 12.1 to 21.2 W t%, and the MgO ranges from 13.1 to 18.1 W t%. The Al_2O_3 content increases in olivine gabbros, whereas dunite and lherzolite show intermediate content levels, and gabbros and gabbronorites show the lowest. Forty-eight analyses of orthopyroxene were taken in lherzolitic peridotite, olivine gabbro and gabbronorite. The general composition shown in Table 3 is Wo: 1.8–4.1, En: 65.8–80.2, Fs: 16.8–31.5 corresponding to bronzitic orthopyroxene and rare grains of hypersthene (Fig. 6-B). The En content in orthopyroxene decreases from lherzolite to gabbronorite to gabbros in agreement with the general trend of differentiation and fractional crystallization. Plagioclases varies in An from 54.6 to 87.9 (Table 4, and Fig. 6-A), according to the expected trend having the highest An values in dunite and olivine bearing gabbronorite (sample P9-36B), followed by lherzolitic peridotite and olivine gabbro. The lowest An content is in gabbros. Some plagioclases crystals are partially weathered (sample 11D-23) and show the lowest An content. From the calculated mean values of An in the plagioclase lherzolitic peridotite, olivine gabbro and some gabbronorite are bytownite (An: 70.1–87.9); in the gabbros and pegmatitic gabbros, the plagioclases are labradorite (An: 54.6–66.8).

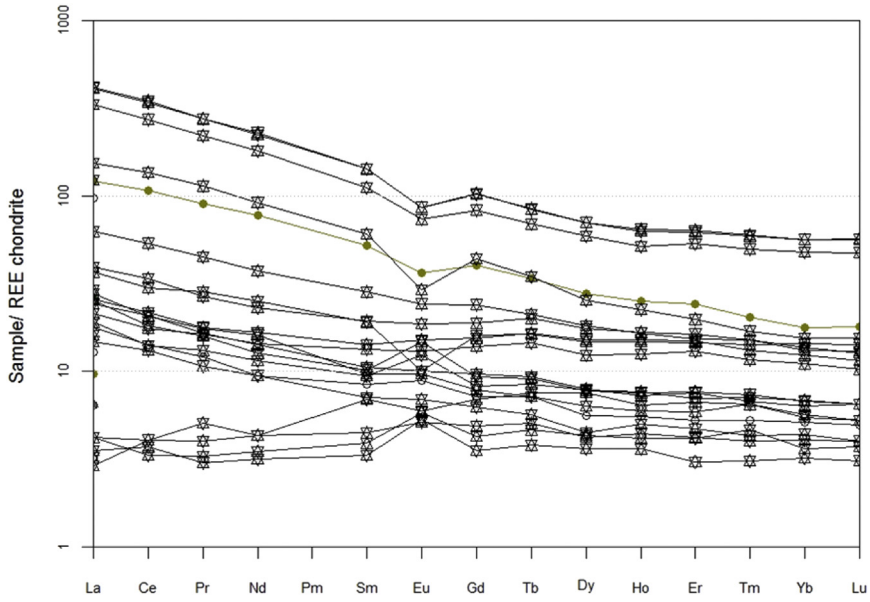

Fig. 8. Chondrite-Normalised Rare Earth Element pattern for the rocks of the Atchiza Intrusion.

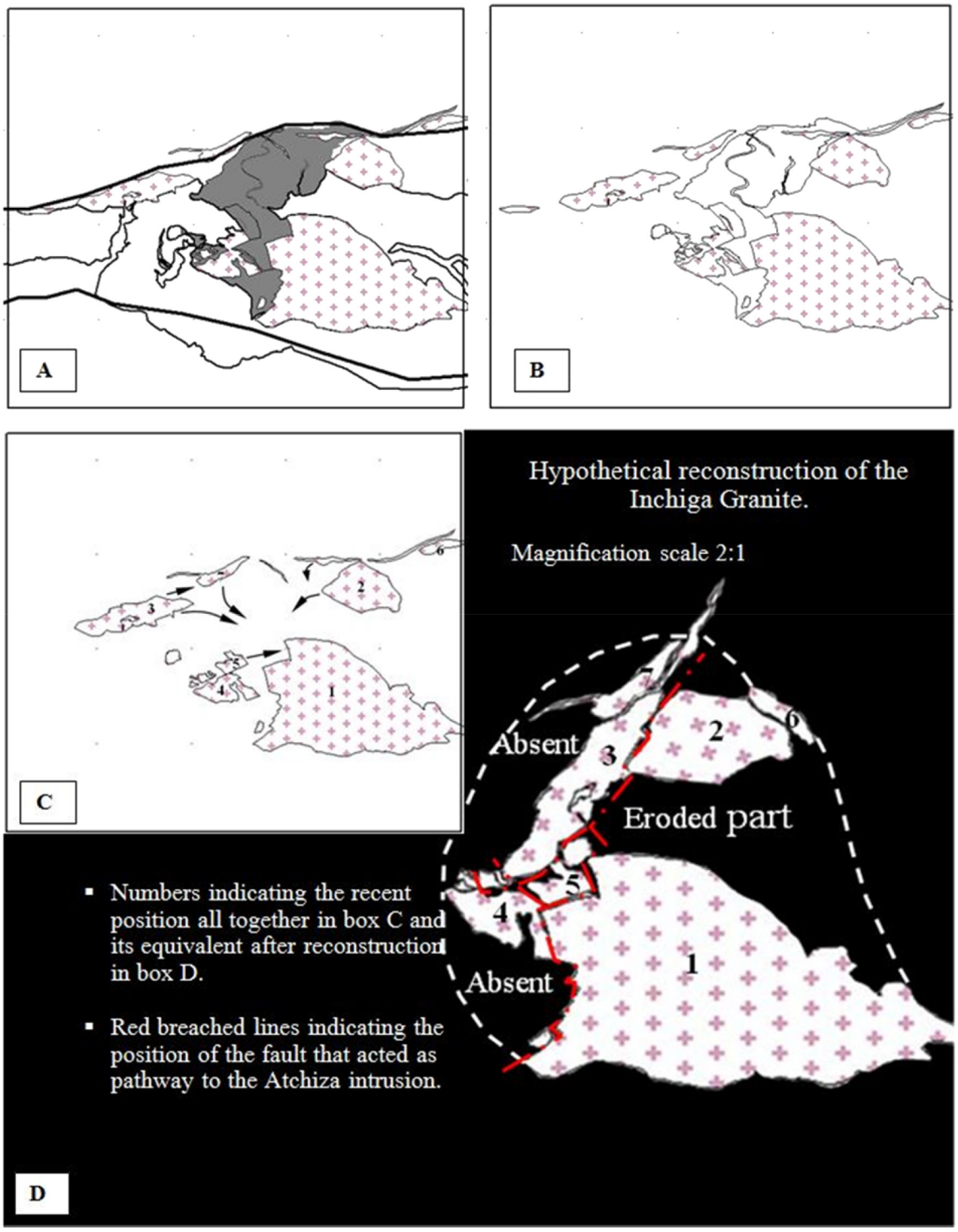

Fig. 9. Hypothetical reconstruction of the Inchiga granite blocks after geology map produced by GTK Consortium (2006). The Inchiga granite is syn-tectonic to other granitic intrusions along the Fínguè Shear Zone dated at 1050 ± 8 Ma. A = Inchiga granite blocks plus the Atchiza Intrusion together (actual situation) in between Fínguè and major Zambezi fault. B = after hollowing up the Atchiza rocks and removal of the faults. C = Removal of the Atchiza limit, numbering the blocks and showing possible movements to fit together. D = final reconstruction of the blocks and possible lines indicating the original body and a fault line cutting through the entire body.

Chromite (ferrichromium) occurs in dunite and lherzolitic peridotite, particularly those with a high olivine percentage (Ol: 76%). The Cr content is in a narrow range from 21.0 to 23.9 W t% and is high in dunite and lherzolitic peridotite and lower in gabbroic rock. Overall, the chromite is low in magnesium (4.1–5.5), chromium (21.0–23.9) and aluminium (9.7–11.5), but has a high iron content (25.8–28.3). The Cr/(Cr + Al) (Cr#) ratio ranges from 0.65 to 0.71 and the MgO/(MgO + FeO) (Mg#) ratio, also in chromite, ranges from 0.63 to 0.79 with the high values in dunite and the lower values in lherzolitic peridotite. A similar trend can be observed when working from ultramafic to mafic rocks.

Table 1
Microprobe analyses of Olivine.

Oxides	Dunite	Lherzolite	Lherzolite	Olivine gabbro	Gabbronorite
	11D_11	11D-12	P10-41	11D-27	P9-36B
	Mean	Mean	Mean	Mean	Mean
SiO_2	40.89	40.41	40.15	39.20	40.79
TiO_2	0.02	0.01	0.00	0.02	0.01
Al_2O_3	0.01	0.02	0.04	0.02	0.03
Cr_2O_3	0.02	0.01	0.01	0.01	0.03
FeO	12.28	12.36	18.76	22.14	12.84
MnO	0.19	0.18	0.27	0.31	0.17
MgO	46.15	45.95	41.05	38.64	45.71
CaO	0.03	0.02	0.02	0.02	0.03
Total	99.59	98.96	100.30	100.36	99.61
End members					
Te	0.20	0.19	0.30	0.35	0.19
Fox	86.80	86.70	79.33	75.39	86.19
Fax	12.96	13.08	20.34	24.23	13.58
Ca-Ol	0.04	0.03	0.03	0.03	0.04
Fe/Mg-Ol	0.27	0.27	0.46	0.57	0.28
Mg#	0.790	0.788	0.686	0.636	0.781
# point	19	8	9	11	3

6. Discussion

6.1. Nature of the primary magma

Rocks of the Atchiza Suite have the chemical characteristics of mafic-ultramafic rocks produced in a continental rift environment that has not evolved to later stages, i.e. the proto-oceanic stage. Petrographic observations show cumulate textures of (a) olivine – chromite in dunite; (b) olivine – (chromite) – clinopyroxene – orthopyroxene in lherzolite together with a lesser amount of plagioclase orthocumulate; and (c) orthopyroxene – clinopyroxene – plagioclase in different types of gabbros with minor amounts of amphibole and biotite. Chilled margins have not be observed. Accordingly, the parent melt composition can only be approximated. However, the data clearly demonstrates that the evolution from ultramafic, through olivine gabbro and norites to gabbro pegmatite is a result of differentiation and fractional crystallization of a mafic parental melt composition. In theory, the parent melt could also be ultramafic, but ultramafic dykes have not observed anywhere in the area.

A possible approach to determine the nature of the primary magma is by using the composition of minerals, notably the Mg/(Mg + Fe) ratio. Of course, using the Mg# of olivine, in particular, may be a poor approach to parent melt compositions since it may easily equilibrate with the more evolved interstitial melts (Paktunc, 1989; Chai and Naldrett, 1992). The calculated Mg# from olivine in dunite and lherzolitic peridotite, respectively, to olivine gabbros shows a considerable decrease, see Fig. 7, (Mg# in Ol_{dunite} 0.786–0.792; in $Ol_{Lherzolite}$ 0.682–0.689 and in $Ol_{Olivine\ gabbros}$ 0.63–0.642).

Ratios of Mg# for pyroxenes show a similar trend as in olivine for the studied rocks (Fig. 7). As shown in the Mg-number vs. SiO_2 plot (Fig. 7), the resulting trend in the three ferro-magnesian silicates exhibit approximately similar patterns where (Mg# from $Cpx_{Lherzolite}$ 0.79; $Cpx_{Oliv.Gabbro}$ 0.68; $Cpx_{gabbronorite}$ 0.66; Cpx_{Gabbro} 0.57) and (Mg# from $Opx_{Lherzolite}$ 0.70; $Opx_{Oliv.Gabbro}$ 0.66; $Opx_{Gabbronorite}$ 0.59; $Opx_{Gabbros}$ 0.57). The Wo (40.8–45.2) content in clinopyroxene decreases from dunite, lherzolite to olivine gabbros. The presented values analysed together with high Fo (75.4–86-8) in the same rocks indicate that the minerals are near-liquid crystallization products of basaltic magma (Azer and El-Gharbawy, 2011). We find the olivine in the Atchiza Suite being more Mg-rich compared with other syn-genetic mafic rocks in the region. For example, the Fo contents in the Atchiza Suite are higher compared with the Munali meta-gabbro in South Zambia where dunite has Fo of 77 W t% (Evans et al., 2005). The Munali meta-gabbro, 300 Km away from the Atchiza Suite, has a similar age (880 Ma (Johnson et al., 2007)) and spatial tectonic relation. When compared to the Tete Gabbro-anorthosite suite in the central-eastern Tete Province, the Atchiza rocks show intermediate Fo contents (Evans et al., 1999).

Sulphide minerals were mainly formed in the later stages of liquid immiscibility between the silicate and sulphide melts, or they simply came to rest in the interstitial spaces of the primocrysts after having passed through the magma column above.

REE Chondrite-normalised patterns of Atchiza rocks are presented in Fig. 8. Some patterns show an enrichment of the Light Rare Earth Elements (LREE) relative to Heavy Rare Earth Elements (HREE). Three distinctive patterns appear from the diagrams: (1) fine-grained gabbro and gabbronorite following a horizontal pattern below 10 times chondrite, (2) medium to coarse-grained gabbro and gabbronorite plotting between 10 and 100 times chondrite and following decreasing trends from LREE to HREE, and (3) coarse-grained and pegmatitic gabbro plotting above 100 times chondrite with the highest decreasing patterns. This systematic evolution of the gabbros implies that the REE contents are a result of differentiation rather than having originated from a different source. The Eu anomaly develops from positive anomalies in the fine-grained to even and negative anomalies in the coarse-grained and pegmatitic gabbro, which suggests the progressive depletion of Eu by fractional crystallization and the removal by plagioclase crystallization (Fig. 8).

6.2. Tectonic framework

Generally, the evolution of the crust in the Zambezi Belt from Mesoproterozoic to Neoproterozoic begins with continental rifting followed by collisional events associated with the Pan-African Orogeny (Porada, 1989; Goscombe et al., 1994; Hanson et al., 1994; Dirks and Sithole, 1999). To the east, the Zambezi Belt is located between the northern margin of the Zimbabwe craton and the south margin of the Congo–Tanzania craton, extending from the western part of the Mozambique Belt to south Zambia. Interpretations vary as to whether the continental collision involved

Table 2
Microprobe analyses of Clinopyroxene.

Oxides	Dunite	Lherzolite		Ol-Gabb		Gabbronorite			Gabbros					Peg. Gab
	11D-11	11D-12	P10-41	11D-27	11D-23	P6-25	P6-23B	P9-36B	11D-02	11D-29	AMO-29	P5-22	11D-32B	11J-11
	Mean	Mean	Mean	Mean	Mean	Mean	Mean	Mean	Mean	Mean	Mean	Mean	Mean	Mean
SiO_2	51.91	52.33	52.79	50.22	49.16	51.79	50.98	51.92	52.30	51.75	52.06	51.85	52.52	48.74
TiO_2	0.48	0.34	0.47	0.66	1.22	0.51	0.32	0.17	0.66	0.72	0.66	0.66	0.65	0.11
Al_2O_3	3.69	3.18	2.82	5.63	4.44	2.72	2.06	4.30	2.19	2.72	2.40	2.31	2.30	1.55
Cr_2O_3	1.21	1.14	0.42	0.02	0.08	0.27	0.20	0.50	0.15	0.17	0.16	0.05	0.02	0.05
FeO	3.99	4.86	5.49	6.98	12.04	7.38	8.90	4.03	11.37	9.28	10.73	10.36	14.31	8.64
MnO	0.12	0.13	0.14	0.14	0.25	0.19	0.23	0.11	0.23	0.21	0.23	0.30	0.37	0.19
MgO	16.07	18.10	15.60	15.12	13.13	14.37	15.88	17.18	15.94	14.25	15.34	13.72	16.01	16.94
CaO	20.98	18.11	21.19	18.81	18.09	19.56	18.52	19.81	17.39	19.62	17.79	20.19	12.69	12.05
Na_2O	0.53	0.41	0.52	0.60	0.46	0.30	0.25	0.50	0.29	0.32	0.28	0.35	0.37	0.14
K_2O	0.01	0.01	0.02	0.10	0.01	0.01	0.00	0.03	0.00	0.01	0.01	0.00	0.02	0.02
Total	98.99	98.61	99.46	98.27	98.88	97.09	97.34	98.58	100.51	99.05	99.65	99.79	99.25	88.45
End members														
Wo	45.16	38.46	44.91	41.94	40.32	43.18	39.62	42.53	36.18	42.02	37.44	42.63	27.50	28.44
En	48.14	53.48	46.01	46.90	40.71	44.12	47.27	51.31	46.15	42.47	44.93	40.32	48.28	55.64
Fs	6.70	8.06	9.08	11.16	18.97	12.71	13.10	6.16	17.67	15.51	17.62	17.05	24.22	15.92
Aegerine	0.00	0.00	0.00	2.25	4.69	0.00	4.34	1.35	2.13	0.00	0.00	0.04	0.00	0.00
Jadeite	4.40	3.94	4.28	3.20	−0.33	2.68	−2.00	3.04	0.75	2.83	2.76	2.98	5.07	2.07
Diopside	95.60	96.07	95.72	94.56	95.65	97.32	97.66	95.61	97.45	97.17	97.24	96.98	94.94	97.93
Mg#	0.80	0.79	0.74	0.68	0.52	0.66	0.64	0.81	0.58	0.61	0.59	0.57	0.53	0.66
# point	10	3	5	4	9	9	6	13	6	11	11	2	4	4

Table 3
Microprobe analyses of Orthopyroxene.

Oxides	Dunite	Lherzolite		Ol-Gabb		Gabbronorite			Gabbros					Peg. Gab
	11D-11	11D-12	P10-41	11D-27	11D-23	P6-25	P6-23B	P9-36B	11D-02	11D-29	AMO-29	P5-22	11D-32B	11J-11
			Values	Mean		Mean	Mean	Mean	Mean	Mean	Mean	Values		
SiO_2			55.37	54.78		53.48	53.89	55.60	54.65	54.12	54.07	55.71		
TiO_2			0.18	0.41		0.25	0.17	0.06	0.21	0.33	0.35	0.20		
Al_2O_3			1.61	1.83		1.48	1.31	1.54	1.25	1.44	1.34	1.06		
Cr_2O_3			0.17	0.03		0.11	0.10	0.27	0.07	0.08	0.10	0.00		
FeO			11.95	14.24		16.47	17.12	10.15	18.17	18.55	18.55	17.86		
MnO			0.29	0.30		0.31	0.33	0.18	0.35	0.36	0.35	0.46		
MgO			28.45	27.21		25.18	24.98	27.17	24.44	24.41	24.56	20.91		
CaO			0.87	1.34		1.11	1.49	1.40	2.05	1.23	1.29	1.20		
Na_2O			0.03	0.04		0.03	0.02	0.03	0.04	0.02	0.02	0.09		
K_2O			0.01	0.01		0.01	0.01	0.03	0.00	0.01	0.01	0.04		
Total			98.92	100.19		98.43	99.42	96.42	101.22	100.56	100.64	97.53		
End members														
Wo			1.75	2.65		2.27	3.00	2.98	4.08	2.48	2.58	2.71		
En			79.52	75.25		71.50	70.07	80.20	67.69	68.37	68.42	65.78		
Fs			18.73	22.09		26.23	26.93	16.82	28.23	29.14	28.99	31.52		
Aegerine			0.00	0.00		0.00	0.00	0.00	0.00	0.00	0.00	0.00		
Jadeite			5.68	5.02		3.91	2.19	3.28	3.41	2.85	2.73	12.20		
Diopside			94.32	94.98		96.09	97.81	96.72	96.59	97.15	97.27	87.80		
Mg#			0.70	0.66		0.60	0.59	0.73	0.57	0.57	0.57	0.54		
# point			1	6		8	8	3	6	7	7	1		

Table 4
Microprobe analyses of Plagioclase.

Oxides	Lherzolite		Ol-Gabb		Gabbronorite			Gabbro					Peg. Gab
	11D-12	P10-41	11D-27	11D-23	P6-25	P6-23B	P9-36B	11D-02	11D-29	AMO-29	P5-22	11D-32B	11J-11
	Mean	Mean	Mean	Mean	Mean	Mean	Mean	Mean	Mean	Mean	Mean	Mean	Mean
SiO_2	49.51	53.38	50.62	54.54	49.39	50.00	46.60	52.05	51.86	51.61	52.96	51.84	48.68
TiO_2	0.05	0.02	0.05	0.07	0.03	0.03	0.01	0.09	0.03	0.04	0.04	0.04	0.02
Al_2O_3	28.31	28.22	30.04	26.81	29.87	30.42	33.10	29.13	29.59	29.44	29.05	28.92	25.59
Cr_2O_3	0.00	0.01	0.01	0.03	0.00	0.00	0.00	0.02	0.00	0.01	0.02	0.01	0.03
FeO	0.24	1.06	0.49	0.95	0.36	0.61	0.24	0.75	0.55	0.59	0.65	1.11	0.06
MnO	0.01	0.04	0.01	0.02	0.01	0.01	0.00	0.01	0.01	0.01	0.01	0.02	0.02
MgO	0.03	0.41	0.04	0.19	0.02	0.15	0.09	0.06	0.06	0.06	0.08	0.35	0.00
CaO	14.50	11.37	14.01	10.71	13.35	14.02	17.45	13.03	13.37	13.29	12.03	11.99	12.41
Na_2O	2.96	4.09	3.03	4.76	3.58	3.27	1.32	3.33	3.53	3.48	4.39	3.06	4.12
K_2O	0.12	0.15	0.26	0.24	0.11	0.06	0.02	0.58	0.25	0.26	0.14	0.42	0.16
Total	95.73	98.76	98.56	98.32	96.71	98.57	98.82	99.05	99.26	98.80	99.36	97.77	91.09
End members													
An	72.53	60.00	70.75	54.60	66.93	70.06	87.86	66.01	66.66	66.80	59.74	66.51	61.87
Ab	26.77	39.04	27.70	43.92	32.44	29.61	12.01	30.51	31.87	31.60	39.41	30.70	37.20
Or	0.70	0.96	1.55	1.48	0.63	0.33	0.13	3.49	1.47	1.58	0.84	2.79	0.95
Mg#	0.11	0.28	0.07	0.16	0.06	0.20	0.27	0.07	0.10	0.09	0.11	0.24	0.03
# point	6	8	7	8	5	10	5	5	9	12	8	8	2

the closure of an oceanic basin, or whether the closure occurred by inversion of an intra-cratonic rift basin.

Considering the presented data, we prefer the idea that the Zambezi Belt underwent a long-lasting period of continental rifting (Oliver et al., 1998; Johnson et al., 2007) and magmatism culminating with a compressional event. Rifting occurred through different episodes such as Katangan (900–850) and Damaran (850–750) (Porada, 1989). The temporal and spatial relationship of the rifting events in the Zambezi Belt corresponds to the first (1100 to 850 Ma) and second (850–750 Ma) events in the Damaran episode. Hence, reactivation of spreading occurred at the beginning of the Katanga episode at ca. 850 Ma. Dirks and Sithole (1999) revised the collisional models and stressed that deformation geometry and kinematic indicators in north-east Zimbabwe were characterised by 800 Ma extensional fabrics; later, this age was refined to 700 Ma (Goscombe et al., 2000). All these data are in agreement with the general model that shows that the rifting in the Zambezi Belt continued until the mid-Neoproterozoic, around 700 Ma, i.e. the Cryogenian period.

6.3. Emplacement of the magma

During the late stage of the Rodinia breakup in the early Neoproterozoic, a connecting fault formed at the western tip of the Fínguè Fault (Fig. 10-B). This connecting fault was created as a result of extensional tectonics controlled by two sub-parallel master faults: the Zambezi Fault and the Fínguè Fault. Such connecting fault systems within different tectonic settings are widely studied (Peacock and Sanderson, 1991; Cruikshank et al., 1991; Kim et al., 2004; Hus et al., 2006). This lateral expansion may be efficient in providing conduits for magma ascent and may explain emplacement of the Atchiza Suite where the Fínguè and Zambezi faults were joined through breaking the Inchiga granite.

The linking fault associated with overall lateral expansion, slab displacement and torsion created room for magma emplacement, i.e. basaltic magma that rose up forming the Atchiza mafic-ultramafic body. This idea is supported by reconstructing the mapped blocks of Inchiga granite (Fig. 9). The isolated blocks, when put together, recreate a single granitic body that was faulted mainly in the NNE-SSW direction (Fig. 9-D). This type of forceful tectonic emplacement is discussed by Brown and Solar (1999) with respect to the emplacement of pluton, where major tectonic structures may have played an important role by creating dilatation space, arresting ascent or controlling the geometry of the pluton. Indeed, the geometry of the Atchiza Suite suggests a tectonic controlled emplacement model, starting from the created connecting fault, to the ascending mafic magma and its emplacement.

Sm–Nd dating of pyroxene gabbro of the Atchiza Suite has yielded an isochron age of 864 ± 30 Ma (GTK Consortium, 2006). A recent SHRIMP age suggests somewhat older ages of 896 ± 6.8 and 890 ± 6.3 Ma. The reported age corresponds to early Neoproterozoic rifting in the Zambezi Belt. The same age was also reported by Dirks et al. (2003) and Goscombe et al. (2000), when referring to igneous rocks of the Masoso and Guro Suite (Marginal Terranes) at the north and north-eastern margins of the Zimbabwe Craton, which yield ages of 870 to 850 Ma, Dirks et al. (2003) respectively.

If the extensional event in the Zambezi Belt continued until ca. 750 Ma and the Finguè Fault is part of this tectonic trend, it may be concluded that the Atchiza Suite being 864 ± 30 Ma was emplaced during an extensional tectonic regime. In addition, the involvement of old LREE-enriched material partially contaminating the Atchiza melts (GTK Consortium, 2006) fits into the phase of early Neoproterozoic rifting in the Zambezi Belt.

The structural geometry of the faults that generated space for the magma argues for a conduit controlled emplacement of the igneous melts. It may support the idea that space was created by the connecting fault opening and torsion alongside the wall rocks. Fault linkage between the Fínguè Fault and the major Zambezi Fault played an important role in this process (Fig. 10). The linking fault breached a part the Inchiga granite body. Brown et al., 2003 discussed this issue with respect to the emplacement of plutons, where major tectonic structures may have played an important role by creating dilatation space, arresting ascent or controlling the geometry of the pluton.

The tectonic setting, age and the structural geometry of the Atchiza Suite imply the following emplacement model:

(1) The Fínguè Fault may suggest a model for the early crustal thinning, extension and basaltic underplating in an ensialic marginal basin;
(2) The older continental crust underwent thinning, and felsic magmatism occurred ca. 1100 Ma at the early stage of the extension (Fig. 10-A);

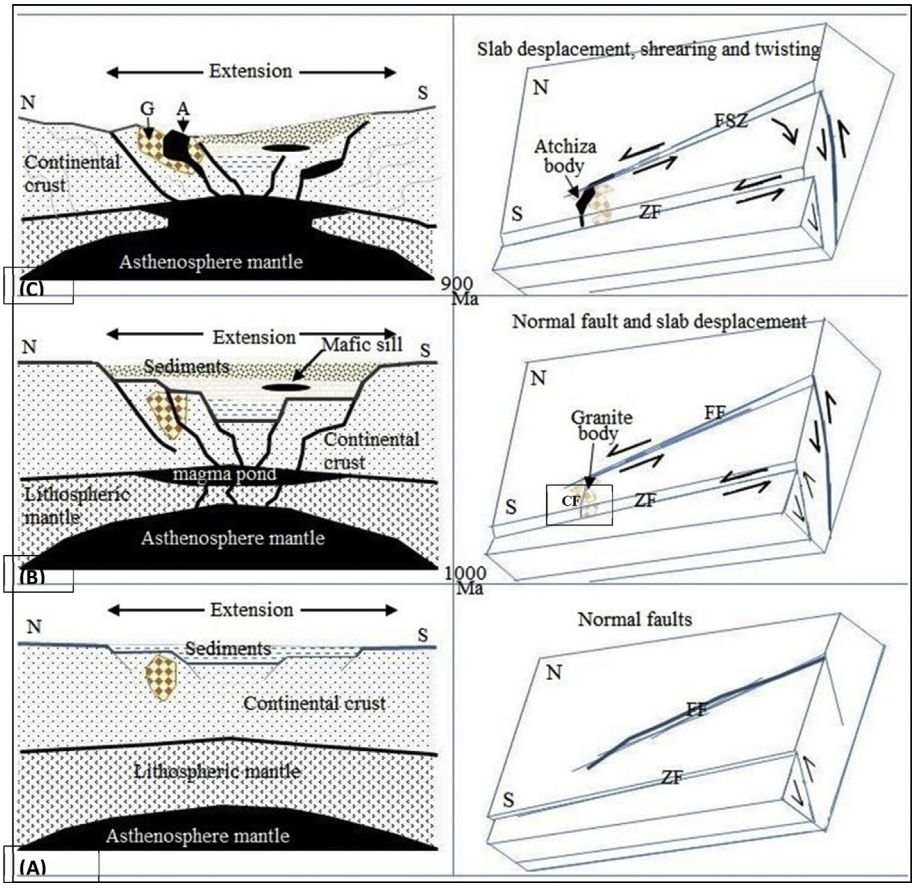

Fig. 10. Sketch of evolution trend giving the essential features of the Zambezi Belt tectonics at the study area in depth and surface perspectives. (A) An early stage of rifting. The starting point of Fínguè Fault (FF); (B) Intermediate phase where mafic magma ascent through the normal faults and the generation of Connecting Fault (CF) between the FF and Zambezi Fault; (C) Continental crust rupture, upwelling of mafic magma and overall accommodation of the blocks and twisting.

(3) The upwelling of asthenospheric mantle melts and the pooling and production of a voluminous magma reservoir at the asthenosphere-lithosphere transition (Fig. 10-B) imposed some buoyant forces that may have caused an accelerated crustal thinning and extension;
(4) Normal faulting and rupturing provided conduits for mafic magma;
(5) Spreading-subsidence of slab rolling-down is a possible mechanism for generation for the Atchiza magma-chamber;
(6) The magma chamber developed due to a resulting force vector imposing torsion of the Inchiga blocks (Fig. 10-C).
(7) Accordingly, the form of the Atchiza intrusion was controlled by an extensional tectonic environment.

7. Conclusions

Based on petrographic observations, mineral composition and REE chondrite-normalised patterns, the following sequence of the magmatic rock formation is suggested: dunite-lherzolitic peridotite-olivine gabbros-gabbronorites-gabbros-pegmatitic gabbro. Olivine and chromite were the first phases, followed by pyroxene and plagioclase, which shows an extensive upward vertical series of magmatic segregation.

Chromite increases in lherzolitic peridotite rock and not in dunite (i.e., chromite crystallized after olivine), which can be explained by the Cr saturation trend after olivine crystallization in ultramafic rocks; however, chromitite layers are not present. Calculated ratios of Mg#, REE patterns and other chemical characteristics favour a magmatic segregation sequential trend from ultramafite to pegmatitic gabbros. Pegmatitic textures were formed due to an increase in volatiles in the magma chamber during the final stage of crystallization.

The mineral chemistry shows that these minerals are near-liquid crystallization products of basaltic magma. Whole rock REE chondrite-normalised patterns show a clear separation of the values on LREE implying that the REE contents in the rocks of the Atchiza Suite are mainly a result of differentiation, but slight crustal contamination/assimilation contributed to the REE contents. In addition, the positive anomaly of Eu in fine-grained gabbros suggests that plagioclase fractionation was important.

The Atchiza mafic-ultramafic layered intrusion resulted from an emplacement of mafic magma in a space created by an extension forces. The space was created through a connecting fault system generated as a result of overall extension, torsion and slab displacement in a rift system. The geometry of the mafic-ultramafic layered body is, thus, tectonically controlled.

Acknowledgements

We gratefully acknowledge the Norwegian Centre for International Cooperation in Higher Education (SIU) through the NUFU Project (NUFUPRO-2007/10120) involving the Norwegian University of Science and Technology (Geology Department-NTNU) and Eduardo Mondlane University (Departamento de geologia – Universidade Eduardo Mondlane-UEM) for financial support for data collection, logistics, living and travel expenses. The Quota Scheme

for students through Norwegian Lånekassen provided partial financial support for travel and living costs. We acknowledge the National Research Fund (Fundo National de Investigação – FNI) of the Mozambican Ministry of Science and Technology (Ministério de Ciência e Tecnologia de Mozambique – MCT) for funding the last period of this doctoral study. Thanks to the Department of Geology at NTNU and SINTEF for allowing us to do the main part of the sample preparation and microprobe analysis, and many other facilities as hosting institutions. The laboratory personnel at the Geology Department of NTNU are thanked for their assistance with getting the polished thin section preparation and microprobe analysis ready on time. Manuscript reviewers are gratefully acknowledged for providing constructive comments.

References

Azer, M.K., El-Gharbawy, R.I., 2011. The neoproterozoic layered mafic-ultramafic intrusion of Gabal Imleih, south Sinai, Egypt: implications of post-collisional magmatism in the north Arabian-Nubian Shield. J. Afr. Earth Sci. 60, 253–272.
Brown, M., Solar, G.S., 1999. The mechanism of ascent and emplacement of granite magma during transpression: a syn-tectonic granite paradigm. Tectonophysics 312, 1–33.
Brown, P.E., Dempster, T.J., Hutton, D.H.W., Becker, S.M., 2003. Extensional tectonics and mafic plutons in the Ketilidian rapakivi granite suite of South Greenland. Lithos 67, 1–13.
Chai, G., Naldrett, A.J., 1992. The Jinchuan intrusion: cumulate of a high-Mg basaltic magma. J. Petrol. 33, 277–303.
Cruikshank, K.M., Zhao, G., Johnson, A.M., 1991. Duplex structure connecting fault segments in entrada sandstone. J. Struct. Geol. 13, 1185–1196.
Dirks, P.H.G.M., Sithole, T.A., 1999. Eclogites in the Makuti gneiss of Zimbabwe: implication for the tectonic evolution of the Zambezi Belt in Southern Africa. J. Metamorph. Geol. 17, 593–612.
Dirks, P.H.G.M., Blenkinsop, T.G., Jelsma, H.A., 2003. The Geological evolution of Africa. Encyclopedia of Life Support Systems (EOLSS), Geology, IV.
Evans, D., Wondrim, D., Johnson, S., Milton, J.A., 2005. Origin of mafic and ultramafic rocks at Munali nickel deposit, Zambia: implications for neoproterozoic mantle evolution in the eastern Africa: abstract. In: Fifth International Dyke Conference 31.7 – 38.2005-Rovaniemi, Finland, p. 14.
Evans, R.J., Ashwal, L.D., Hamilton, M.A., 1999. Mafic, ultramafic, and anorthositic rocks of the Tete Complex, Mozambique; petrology, age, and significance. South Afr. J. Geol. 102, 153–166.
Ferreira Filho, C.F., Pimentel, M.M., De Araujo, S.M., Laux, J.H., 2010. Layered intrusions and volcanic sequences in central Brazil: geological and geochronological constraints for Mesoproterozoic (1.25 Ga) and neoproterozoic (0.79 Ga) igneous association. Precambrian Res. 183, 617–634.
Goscombe, B., Pey, P., Both, F., 1994. Structural evolution of the Chewore Inliers, Zambezi Belt, Zimbabwe. J. Afr. Earth Sci. 19, 199–224.
Goscombe, B., Armstrong, R., Barton, J.M., 2000. Geology of the Chewore Iliers, Zimbabwe: constraining the Mesoproterozoic to Palaeozoic evolution of the Zambezi Belt. J. Afr. Earth Sci. 30, 589–627.
GTK Consortium, 2006. Map Explanation. In: Sheets 1430 – 1432 and 1530 – 1534. Geology of Degree Sheets Inhamambo, Maluwera, Chifunde, Zumbo, Fíngoè-Mágoè, Songo, Cazula and Zóbuè, Mozambique, vol. 4. Ministério dos Recursos Minerais, Direcção Nacional de Geologia, Mozambique.
Hanson, R.E., Wilson, T.J., Munyanyiwa, H., 1994. Geologic evolution of the neoproterozoic Zambezi Orogenic Belt in Zambia. J. Afr. Earth Sci. 18, 135–150.
Hus, R., De Batist, M., Klerkx, J., Matton, C., 2006. Fault linkage in continental rifts: structural and evolution of a large relay ramp in Zavarotny; Lake Baikal (Russia). J. Struct. Geol. 28, 1338–1351.
Johnson, S.P., De Waele, B., Evans, D., Banda, W., Tembo, R., Milton, J.A., Tani, K., 2007. Geochronology of the Zambezi supracrustal sequence, southern Zambia: a record of neoproterozoic divergent process along the southern margin of the Congo craton. J. Geol. 115, 355–374.
Johnson, S.P., Oliver, G.J.H., 2004. Tectonothermal history of the Kaourera Arc, northern Zimbabwe: implications for the tectonic evolution of the Irumide and Zambezi Belts of south central Africa. Precambrian Res. 130, 71–97.
Kim, Y.-S., Peacock, D.C.P., Sanderson, D.J., 2004. Fault damage zones. J. Struct. Geol. 26, 503–517.
Kröner, A., Stern, R.J., 2004. Pan-African Orogeny. Encyclopaedia of Geology, 1. Elsevier, Amsterdam.
Maier, W.D., Groves, D.I., 2011. Temporal and spatial control on the formation of magmatic PGE and Ni-Cu deposits. Min. Deposita 46, 841–857.
Oliver, G.J.H., Johnson, S.P., Williams, I.S., Herd, D.A., 1998. Relict 1.4 Ga oceanic crust in the Zambezi Valley, northern Zimbabwe: evidence of Mesoproterozoic supercontinental fragmentation. Geol. J. 26, 571–573.
Paktunc, A.D., 1989. Petrology of the St. Stephen intrusion and the genesis of related nickel-copper sulphide deposits. J. Econ. Geol. 84, 817–840.
Peacock, D.C.P., Sanderson, D.J., 1991. Displacements, segment linkage and relay ramps in normal fault zones. J. Struct. Geol. 13, 721–733.
Pereira, M.F., Castro, A., Chichorro, M., Fernández, C., Daz-Alvarado, J., Mart, J., Rodriguez, C., 2014. Chronological link between deep-seated processes in magma chambers and eruptions: permo-carboniferous magmatismo in the core of Pangaea (south Pyrenees). Gondwana Res. 25, 290–308.
Poldervaart, A., Hess, H.H., 1951. Pyroxene in the crystallization of basaltic magma. J. Geol. 59, 472–489.
Porada, H., 1989. Pan-African orogenesis in southern to equatorial Africa and eastern Brazil. Precambrian Res. 44, 103–136.
Real, F., 1962. O maciço ultrabásico do Monte Atchiza (Moçambique). Reconhecimento geológico-mineiro. Junta de Investigação do Ultramar. DNG Library No. 1023.
Stern, R.J., 1994. Arc assembly and continental collision in the neoproterozoic east Africa orogeny: implications for the consolidation of Gondwanaland. Annu. Rev. Earth Planet. Sci. 22, 319–351.
Streckeisen, A., 1976. To each plutonic rock its proper name. Earth-Science Rev. 12, 1–33.
Vasconcelos, P., Hall, T.C.P., 1948. Geologia de Moçambique. Agência Geral das Colonias, Biblioteca da Direcção Nacional de Geologia, Maputo, Moçambique.
Westerhof, A.B., Lehtonen, M.I., Mäkitie, H., Manninen, T., Pekkala, Y., Gustafsson, N.,B., Tohon, A., 2008. The Tete-Chipata Belt: a new multiple terrane element from western Mozambique and southern Zambia. Geol. Surv. Finl. Special Pap. 48, 145–166.

Further reading

Hall, A., 1996. Igneous Petrology, second ed. Addison Wesley Longman Limited, Edimburgh Gate, Harlow, p. 462.
Yoshiro, T., Okudaira, T., 2004. Crustal growth by magmatic accretion constrained by metamorphic P-T paths and thermal models of the Kohistan Arc, NW Himalayas. J. Petrol. 45, 2287–2303.